Microwave-induced phase escape in a Josephson tunnel junction

Sun Guozhu,[1,*] Wang Yiwen,[2] Cao Junyu,[1] Chen Jian,[1] Ji Zhengming,[1] Kang Lin,[1] Xu Weiwei,[1] Yu Yang,[2] Han Siyuan,[1,3] and Wu Peiheng[1]

[1]*Research Institute of Superconductor Electronics, Department of Electronic Science and Engineering, Nanjing University, Nanjing 210093, People's Republic of China*

[2]*National Laboratory of Solid State Microstructures, Department of Physics, Nanjing University, Nanjing 210093, People's Republic of China*

[3]*Department of Physics and Astronomy, University of Kansas, Lawrence, Kansas 66045, USA*

(Received 2 November 2007; revised manuscript received 7 January 2008; published 28 March 2008)

We perform both theoretical and experimental investigations on the phase escape of a current-biased Josephson tunnel junction under microwave irradiation. The switching current distributions exhibit abundant nonlinear behaviors depending on the power and frequency of the applied microwave. We present a model to describe the behavior of the primary peak in the switching current distribution, which is confirmed by our experimental results. The obtained features can be used to characterize the damping parameter of Josephson junctions.

DOI: 10.1103/PhysRevB.77.104531 PACS number(s): 74.50.+r, 03.65.Sq, 05.45.−a

Josephson junctions are very important nonlinear systems for both fundamental researches and practical applications. Driving these nonlinear systems with microwave produce enormous interesting phenomena such as Shapiro steps and photon-assisted tunneling.[1,2] So far, many useful applications based on the microwave driven junctions have already been developed. Moreover, recent investigation on the quantum computing in Josephson junction devices has opened another vigorous area for this topic. Many kinds of superconducting Josephson qubits[3] have been proposed and demonstrated. In those superconducting qubits, Josephson junctions are the key elements and microwave irradiation is crucial to perform the qubits' control and readout.

Therefore, it is mandatory to thoroughly understand both the classical and quantum dynamics of the microwave driven Josephson junctions. Theoretical and experimental works[4–7] have been conducted, in which a lot of attractive characteristics have been reported. In this paper, we present here some phenomena of the phase escape in a microwave driven Josephson tunnel junction. The switching current distribution $P(I_s)$ under microwave irradiation shows a qualitative difference when microwave power and frequency vary. We develop a quantitative model based on the classical dynamics to understand the experimental results. Our model also shows the effect of the damping parameter on the junction's phase escape. Therefore, using this model, we can experimentally determine the junction damping parameter, which is an important parameter while difficult to obtain.

The equation of motion of a current-biased Josephson tunnel junction is identical to that of a particle moving in a washboard potential [shown in Fig. 1(a)],

$$\frac{\hbar C}{2e}\ddot{\theta}(t) + \frac{\hbar}{2eR}\dot{\theta}(t) + I_0 \sin\theta = I_b, \tag{1}$$

where θ is the phase difference across the junction and corresponds to the coordinate of the phase particle. C and R are the shunt capacitance and resistance, respectively. I_b is the bias current and I_0 is the critical current. For I_b, slightly smaller than I_0, the potential has a series of metastable wells with barrier height given by $\Delta U = 2E_J(\sqrt{1-(i_{dc})^2} - i_{dc}\cos^{-1}(i_{dc}))$. Here, $E_J = I_0\Phi_0/2\pi$, $i_{dc} = I_b/I_0$, and $\Phi_0 \equiv h/2e$. A particle initially trapped in a potential well (corresponding to a zero voltage drop across the junction) oscillates at the bottom of the well with the plasma frequency $\omega_p = \omega_{p0}[1-(i_{dc})^2]^{1/4} \equiv (2\pi I_0/C\Phi_0)^{1/2}[1-(i_{dc})^2]^{1/4}$. Thermal or quantum fluctuation can kick the particle out of the potential well to a voltage state. The current where the junction switches from zero to finite voltage is called switching current (I_s). Since junction switching is a random process, the

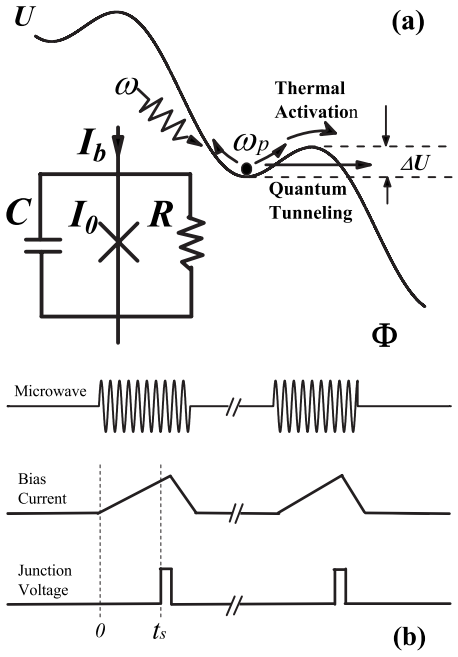

FIG. 1. (a) Washboard potential and equivalent circuit (inset) of a current-biased Josephson tunnel junction with $I_b < I_0$. (b) Schematic time profile for measuring the switching current distribution $P(I_s)$ of a Josephson junction with or without microwave irradiation.

switching current distribution $P(I_s)$ contains all useful information and can be used to investigate classical and quantum dynamics. To build $P(I_s)$ experimentally, we sweep the bias current from zero to I_0 and repeatedly measure the switching. A peak with mean switching current value slightly smaller than I_0 can be observed in $P(I_s)$. We hereafter name this peak as the primary peak, which is caused by either the thermal activation or quantum tunneling. If we drive the junction using a continuous microwave with appropriate frequency and power, there will be an enhancement of the escape from the potential well, which manifests itself by a resonant peak besides the primary peak in $P(I_s)$. This is known as the microwave induced double-peak structure.[4–7] The positions of the primary peak and the resonant peak are denoted as I_p and I_r, which are the current values of two maxima, respectively.

The resonant peak is predicted in both classical and quantum dynamics. Qualitatively speaking, at high temperature, the junction is in the classical regime. When the driving frequency equals to the plasma frequency, the classical resonance occurs. Therefore, the particle has the largest oscillation amplitude in the potential well and the escape is enhanced. At low temperature, especially lower than the crossover temperature T^* ($T^*=\hbar\omega_{p0}/2\pi k_B$, where k_B is Boltzmann's constant), the energy levels in the potential well become quantized. The quantum tunneling dominates over the thermal activation. When microwave frequency matches the energy difference between the energy levels, it will pronouncedly increase the population of the excited state, in which the tunneling from the well is much easier.[8–11] Consequently, the resonant peak appears in the switching current distribution. In cubic approximation of the potential, the energy differences between the lowest two energy levels are determined by[12] $\omega_{01}=\omega_p[1-(5/36)(\hbar\omega_p/\Delta U)]$. Similar to that in the microscopic quantum systems, such a process is also applicable to the multiphoton absorption for $n\omega=\omega_{01}$; here n is the number of photons absorbed in the transitions. Some interesting phenomena will appear in the behavior of the resonant peak when the defects in the tunnel barrier couple to the energy levels of the qubits, which have been reported by other groups.[13–15]

Our work focuses on the behavior of the primary peak under microwave irradiation. For a weak microwave power, the potential of the junction is almost unperturbed by microwave irradiation. It is very easy to enhance the population in the excited state. Therefore, only single photon absorption is observed in this process and the position of the primary peak exhibits almost no change compared to that without microwave irradiation. For a strong microwave power, multiphoton absorption occurs. Under such high power irradiation, the potential is strongly perturbed and suppressed. The phase of the junction escapes from the well much more easily, which means the position of the primary peak will move to a lower value along the bias current axis.

A semiquantitative model based on the classical equation of motion can be used to describe the behavior of the primary peak. With microwave irradiation presence, we add $I_{mw}\sin\Omega t$ on the right hand side of Eq. (1), where Ω is microwave frequency and I_{mw} represents amplitude of microwave-induced alternating current flowing through the junction. For convenience, we rewrite the equation of motion in a normalized form as

$$\ddot{\theta}(\tau)+\alpha\dot{\theta}(\tau)+\sin\theta=i_{dc}+i_{mw}\sin\omega\tau, \tag{2}$$

where $\alpha=\hbar\omega_{p0}/2eRI_0$ is the damping parameter. Other rescaled parameters are $\tau=t/\omega_{p0}^{-1}$, $i_{dc}=I_b/I_0$, $i_{mw}=I_{mw}/I_0$, and $\omega=\Omega/\omega_{p0}$. For a weak damping system and small microwave amplitude, $\alpha\ll 1$ and $i_{mw}\ll 1$.

For a slowly varying bias current, it is a good approximation to separate θ in Eq. (2) into two terms: an equilibrium position term φ_0 ($i_{dc}=\sin\varphi_0$) and a quickly oscillating term $\varphi(\tau)$ around φ_0. Inserting $\theta=\varphi_0+\varphi(\tau)$ into Eq. (2) yields the dynamic equation for $\varphi(\tau)$, which can be Taylor expanded in powers of $\varphi(\tau)$ as long as the oscillation amplitude of $\varphi(\tau)$ is small. Up to order of $\varphi^2(\tau)$, we obtain the nonlinear dynamic equation,

$$\ddot{\varphi}(\tau)+\alpha\dot{\varphi}(\tau)+\sqrt{1-i_{dc}^2}\varphi(\tau)-\frac{i_{dc}}{2}\varphi^2(\tau)=i_{mw}\sin\omega\tau. \tag{3}$$

The standard relationship between the normalized resonance frequency and bias current reads $\omega_r=(1/n)(\omega_p/\omega_{p0})=(1/n)(1-i_{dc}^2)^{1/4}$ ($n=1,2,3,\ldots$). To observe both the primary peak and the resonant peak, the amplitude of microwave should be tuned to a very narrow regime, which is defined as $i_{crmw}(\omega_r)$ in this paper. From the classical point of view, $i_{crmw}(\omega_r)$ is actually the critical microwave amplitude, which can provide a suitable energy necessary for the phase particle to resonantly escape from the potential well. Above (below) $i_{crmw}(\omega_r)$, only the resonant peak (the primary peak) shows up in the switching distribution [i.e., no double-peak $P(I_s)$ can be observed when $i_{mw}\neq i_{crmw}(\omega_r)$].

In the following section, we calculate $i_{crmw}(\omega_r)$ for the harmonic ($n=1$) and nth-subharmonic resonances ($n=2,3,4$).

$n=1$. By retaining only the linear term of $\varphi(\tau)$ in Eq. (3), we obtain

$$\ddot{\varphi}(\tau)+\alpha\dot{\varphi}(\tau)+\sqrt{1-i_{dc}^2}\varphi(\tau)=i_{mw}\sin\omega\tau. \tag{4}$$

The stationary solution to this linearly forced oscillation equation is given by

$$\varphi^{(1)}(\tau)=A\cos(\omega\tau+\delta_1),$$

where δ_1 is a phase constant and $A=i_{mw}/\sqrt{(\sqrt{1-i_{dc}^2}-\omega^2)^2+\alpha^2\omega^2}$ represents the steady oscillation amplitude. In the case of resonance, $\omega_r=(1-i_{dc}^2)^{1/4}$, the resonance amplitude $A_r=i_{mw}/\alpha\omega_r$. By equating A_r to the phase distance between the stable phase position φ_0 and the location of the primary peak i_p ($i_p=I_p/I_0$), we are able to obtain $i_{crmw}^{(1)}(\omega_r)=\alpha\omega_r(\arcsin i_p-\arcsin i_{dc})$. It is evident that the critical microwave amplitude for $n=1$ can be quite small provided that the damping is weak, which is the case in our experiment.

$n=2$. We now consider the stationary solution of a 2ω mode to Eq. (3), namely, $\varphi(\tau)=\varphi^{(1)}(\tau)+\varphi^{(2)}(\tau)$, in which $\varphi^{(2)}(\tau)=B\cos(2\omega\tau+\delta_2)$, with δ_2 as a phase constant and B as the oscillation amplitude. Inserting $\varphi(\tau)$ into Eq. (3) produces

$$\ddot{\varphi}^{(2)}(\tau) + \alpha\dot{\varphi}^{(2)}(\tau) + \sqrt{1-i_{dc}^2}\varphi^{(2)}(\tau) = \frac{i_{dc}}{4}A^2\cos(2\omega\tau + 2\delta_2) + \text{other terms}. \quad (5)$$

We are justified to neglect other terms since the first term dominates the dynamics of $\varphi^{(2)}(\tau)$. We can then easily obtain the oscillation amplitude for the 2ω mode,

$$B \cong \frac{A^2 i_{dc}/4}{\sqrt{[\sqrt{1-i_{dc}^2}-(2\omega)^2]^2+\alpha^2(2\omega)^2}}.$$

For $\omega_r = \frac{1}{2}(1-i_{dc}^2)^{1/4}$, the resonance amplitude $B_r = [(i_{dc}/4)/2\alpha\omega_r][i_{mw}^2/(\sqrt{1-i_{dc}^2}-\omega_r^2)^2+\alpha^2\omega_r^2]$ We can then estimate $i_{crmw}^{(2)}(\omega_r) \cong 6\omega_r^2[i_{crmw}^{(1)}(2\omega_r)/i_{dc}]^{1/2}$, indicating that a larger microwave amplitude is required to trigger a 2ω-mode resonance compared to that for the ω-mode resonance.

$n=3$ and $n=4$. Similar to the previous analysis, by writing the solution of Eq. (3) as a 3ω-mode solution and 4ω-mode solution, we obtain $i_{crmw}^{(3)}(\omega_r) \cong 8(40\omega_r^8)^{1/3} \times [i_{crmw}^{(1)}(3\omega_r)/i_{dc}^2]^{1/3}$ with the resonance condition $\omega_r = \frac{1}{3}(1-i_{dc}^2)^{1/4}$ and $i_{crmw}^{(4)}(\omega_r) \cong 30(84)^{1/4}\omega_r^3[i_{crmw}^{(1)}(4\omega_r)/i_{dc}^3]^{1/4}$ with the resonance condition $\omega_r = \frac{1}{4}(1-i_{dc}^2)^{1/4}$, respectively.

Note that as we derive the above expressions, the thermal current noise is neglected. We should expect that the presence of thermal fluctuations will shift the critical amplitude of microwave to a slightly smaller value.

In the absence of microwave as well as thermal fluctuations, the potential energy of the Josephson junction is $U_0(\varphi_0) = -E_J[(I_b/I_0)\varphi_0 + \cos\varphi_0]$ and I_p equals I_0. However, in the presence of microwave radiation, the potential energy of the Josephson junction is effectively suppressed as[16]

$$U_{eff}(\varphi_0, i_{mw}, \omega) = -E_J\left[\frac{I_b}{I_0}\varphi_0 + \cos\varphi_0\left(1 - \frac{i_{mw}^2/2}{(\cos\varphi_0-\omega^2)^2+\alpha^2\omega^2}\right)\right]. \quad (6)$$

When the resonance condition is satisfied, i_p is subsequently shifted down to

$$i_p = 1 - \frac{i_{crmw}^2(\omega_r)/2}{(\sqrt{1-i_p^2}-\omega_r^2)^2+\alpha^2\omega_r^2}. \quad (7)$$

Note here we have neglected the n dependence of $i_{crmw}(\omega_r)$. The presence of thermal fluctuations will simply decrease I_p, which can be written as[4]

$$i_p = 1 - \langle\delta i_p(T)\rangle - \frac{i_{crmw}^2(\omega_r)/2}{(\sqrt{1-i_p^2}-\omega_r^2)^2+\alpha^2\omega_r^2}, \quad (8)$$

where $\langle\delta i_p(T)\rangle = [(k_BT/2E_J)\ln(\omega_0 I_0/2\pi\dot{I}_b)]^{2/3}/I_0$ is the shift of i_p due to thermal fluctuations at temperature T and $\dot{I}_b$ is the ramp rate of the bias current. As we have determined $i_{crmw}(\omega_r)$ already, by solving transcendental Eq. (8) for i_p, we obtain I_p. By using this model, we calculated the position of the primary and resonant peaks in a typical $P(I_s)$, as shown in Fig. 2. The damping parameters are chosen to be $\alpha = 0.002$ and $\alpha = 0.2$. The sample parameters we used are $I_0 = 36.08\ \mu$A, $C = 5.8$ pF, and $T = 80$ mK. As we can see, the curvature of the primary peak is closely related to α and n. In the case of weak damping ($\alpha = 0.002$), I_p for $n=1$ is nearly a constant and just slightly suppressed for $n=2$, 3, and 4. This is reasonable. Since the critical microwave power for a subharmonic resonance is larger than that for a harmonic resonance, consequently the phase particle "sees" a more suppressed potential barrier. In the case of stronger damping ($\alpha = 0.2$), I_p for $n=1$ is also slightly lowered, while for $n=2$, 3, and 4, I_p is heavily suppressed. This indicates that a larger critical microwave power is required for a higher damping system, leading to a larger suppression of the potential barrier.

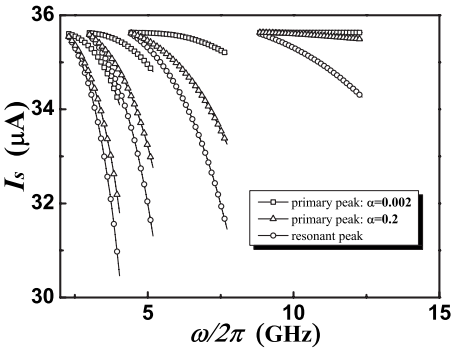

FIG. 2. Dependence of the location of the primary and resonant peaks (circles) on microwave frequency for $\alpha = 0.002$ (squares) and $\alpha = 0.2$ (triangles) based on the presented model in the text.

The experimental results quantitatively agree with the prediction of our model. The sample is a $10\times10\ \mu m^2$ $Nb/AlO_x/Nb$ Josephson tunnel junction fabricated with a standard trilayer process. This junction has a critical current of $I_0 = 36.08\ \mu$A and an effective capacitance of $C = 5.8$ pF, determined from independent measurements.[17] The sample is mounted on a chip carrier enclosed in a superconducting aluminum sample cell. The assembly is put in the dilution refrigerator and magnetically shielded by three layers of Mumetal cylinders surrounding the dewar at room temperature. All electrical leads that connect the junction to room temperature electronics are carefully filtered by *RC* filters and Cu-powder filters. Battery-powered low-noise preamplifiers are used for all measurements. Microwave can be injected via a separate coaxial cable, which is capacitively coupled to the junction. A 20 dB attenuator at the 1 K stage, a 10 dB attenuator, and a dc block at the 600 mK stage are used to reduce the external noise. In general, $P(I_s)$ is obtained using the time-of-flight technique [shown in Fig. 1(b)]: For each escape event, with microwave irradiation always on, we start the cycle by ramping up the bias current linearly from zero to a value slightly higher than I_0. The junction is sure to escape from the potential well because when $I_b > I_0$, there is no potential well at all. This escape generates a zero-voltage to finite-voltage jump across the junction which triggers the timer to record a switching time t_s. Then, the bias current I_b is gradually reduced to zero, resetting the junction to the zero-voltage state. This process is repeated 5.0×10^3 times to obtain an ensemble of t_s. Having known the ramping rate $\dot{I}_b$, we obtain an ensemble of I_s and thus $P(I_s)$. Microwave with frequency between 2.5 and 20 GHz is applied to the sample.

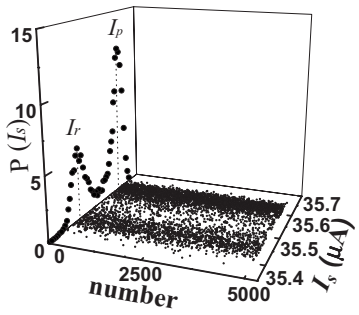

FIG. 3. Raw data of the switching current (I_s) with microwave irradiation (nominal power: −22.20 dBm and $\omega/2\pi$=9.300 GHz) and the corresponding stochastic switching current distribution $P(I_s)$. I_p and I_r denote the location of the primary peak and the resonant peak, respectively.

For all the measurements, the temperature is 16 mK, which is significantly below the classical-to-quantum crossover temperature (T^*=80 mK) of our junction.

In Fig. 3, on the x-y plane we show the raw data of the switching current with microwave irradiation (nominal power: −22.20 dBm and $\omega/2\pi$=9.300 GHz). Shown on the x-z plane is the corresponding stochastic distribution $P(I_s)$. The double-peak structure containing the primary peak and the resonant peak is observed as expected.

Figure 4 shows the three-dimensional (3D) plot of the selected distributions with the double-peak structure in the whole range of microwave frequency. Note that microwave power for each double-peak structure distribution is different. We have observed two typical types of double-peak structure in the experiments. The first one is shown in Fig. 5(a). Because the damping of our system is low, microwave power for harmonic resonance is low. As we can see, although the height of the primary peak decreases as microwave power increases, its position remains almost unchanged. Yet, the other one is shown in Fig. 5(b), in which both the position and height of the primary peak move to lower values with the increase of microwave power because higher microwave power is needed for subharmonic resonance as discussed above.

Inserting the experimentally determined parameters in the model, we calculate the dependence of I_p on microwave frequency. From the best fitting to the experimental data, we get α=0.08. In Fig. 6, we plot the dependence of I_p (circles) and I_r (squares) on microwave frequency in two dimensions. The theoretical I_r are plotted in red lines. The dependence of I_r on

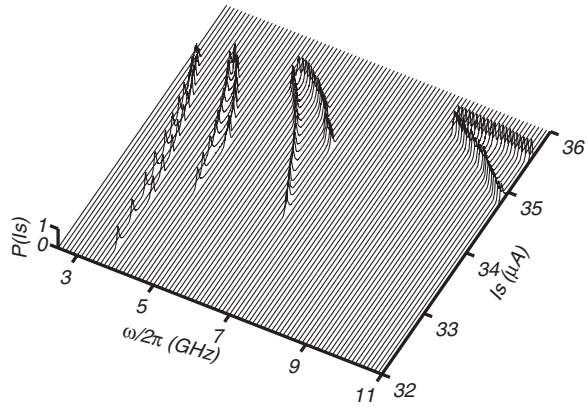

FIG. 4. 3D plot of the double-peak structure.

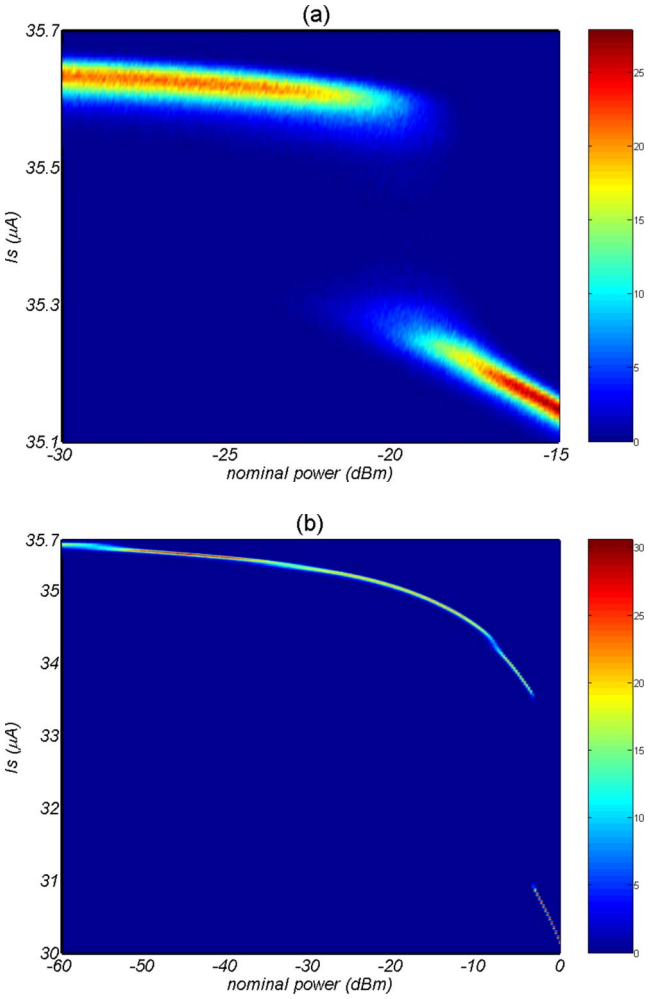

FIG. 5. (Color online) Density plot of $P(I_s)$ versus the applied microwave power at 16 mK in two typical types of double-peak structure. (a) $\omega/2\pi$=9.950 GHz and (b) $\omega/2\pi$=8.000 GHz.

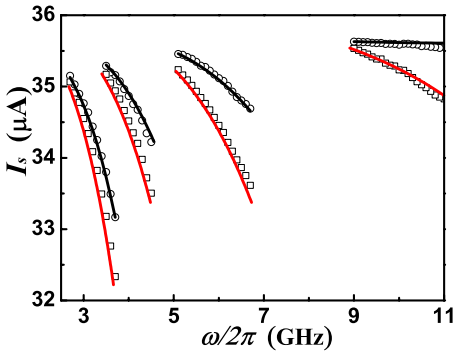

FIG. 6. (Color online) Dependence of the location of the primary and resonant peaks in $P(I_s)$ on microwave frequency at 16 mK: red lines for the theoretical resonant peak, black lines for the theoretical primary peak, squares for the experimental resonant peak, and circles for the experimental primary peak.

the microwave frequency is in good accord with the experimental result. The theoretical I_p based on the above model are plotted in black lines, which also show good agreement with the experimental ones. The small difference between them is caused by the approximation in the model and/or the α's frequency dependence.[9]

A direct application of our analysis is that we can determine the damping parameter α experimentally. The damping parameter is important for superconducting qubits because junctions are widely used as qubit element and readout devices. However, it is usually difficult to measure α since it depends on many factors such as the qubit design, measurement setup, junction fabrication, and temperature.

In conclusion, we have carried out not only the experimental measurement but also theoretical analysis of the phase escape in a current-biased Josephson junction under microwave irradiation. The switching current distribution $P(I_s)$ manifests itself by different behaviors depending on the power and frequency of the applied microwave irradiation. Two typical types of double-peak structure are observed. Both the primary peak and the resonant peak are strongly related to the damping parameter, the microwave power, the microwave frequency, and the photon absorption process. We have successfully developed a model to explain the behavior of the primary peak in these double-peak structures. The model is useful to determine the damping parameter of the system.

This work is partially supported by NSFC (Grant Nos. 10704034, 10674062, 10534060), by the State Key Program for Basic Research of China (Grant Nos. 2007CB310404, 2006CB921801, and 2006CB601006), by the 111 project under Grant No. B07026, by the Natural Science Foundation of Jangsu Province (Grant No. BK2006118), and by the Doctoral Funds of Ministry of Education of the People's Republic of China (Grant No. 20060284022).

*gzsun@nju.edu.cn

[1] S. Shapiro, Phys. Rev. Lett. **11**, 80 (1963).
[2] M. Tinkham, *Introduction to Superconductivity*, 2nd ed. (McGraw-Hill, New York, 1996).
[3] Yu. Makhlin, G. Schön, and A. Shnirman, Rev. Mod. Phys. **73**, 357 (2001).
[4] M. V. Fistul, A. Wallraff, and A. V. Ustinov, Phys. Rev. B **68**, 060504(R) (2003).
[5] A. Wallraff, T. Duty, A. Lukashenko, and A. V. Ustinov, Phys. Rev. Lett. **90**, 037003 (2003).
[6] N. Grønbech-Jensen, M. G. Castellano, F. Chiarello, M. Cirillo, C. Cosmelli, L. V. Filippenko, R. Russo, and G. Torrioli, Phys. Rev. Lett. **93**, 107002 (2004).
[7] G. Rotoli, T. Bauch, T. Lindstrom, D. Stornaiuolo, F. Tafuri, and F. Lombardi, Phys. Rev. B **75**, 144501 (2007).
[8] J. M. Martinis, M. H. Devoret, and J. Clarke, Phys. Rev. B **35**, 4682 (1987).
[9] J. M. Martinis, S. Nam, J. Aumentado, and C. Urbina, Phys. Rev. Lett. **89**, 117901 (2002).
[10] Y. Yu, S. Han, X. Chu, S. Chu, and Z. Wang, Science **296**, 889 (2002).
[11] A. J. Berkley, H. Xu, M. A. Gubrud, R. C. Ramos, J. R. Anderson, C. J. Lobb, and F. C. Wellstood, Phys. Rev. B **68**, 060502(R) (2003).
[12] A. J. Berkley, Ph.D. thesis, University of Maryland, 2003.
[13] K. B. Cooper, Matthias Steffen, R. McDermott, R. W. Simmonds, Seongshik Oh, D. A. Hite, D. P. Pappas, and John M. Martinis, Phys. Rev. Lett. **93**, 180401 (2004).
[14] R. W. Simmonds, K. M. Lang, D. A. Hite, S. Nam, D. P. Pappas, and John M. Martinis, Phys. Rev. Lett. **93**, 077003 (2004).
[15] J. M. Martinis, K. B. Cooper, R. McDermott, Matthias Steffen, Markus Ansmann, K. D. Osborn, K. Cicak, Seongshik Oh, D. P. Pappas, R. W. Simmonds, and Clare C. Yu, Phys. Rev. Lett. **95**, 210503 (2005).
[16] M. V. Fistul and A. V. Ustinov, Phys. Rev. B **63**, 024508 (2000).
[17] G. Z. Sun, J. Chen, Z. M. Ji, W. W. Xu, L. Kang, P. H. Wu, N. Dong, G. F. Mao, Y. Yu, and D. Y. Xing, Appl. Phys. Lett. **89**, 082516 (2006).